A Selective and Purification-Free Strategy for Labeling Adherent Cells with Inorganic Nanoparticles

Gao, Yu; Lim, Jing; Yeo, David Chen Loong; Liao, Shanshan; Lans, Malin; Wang, Yaqi; Teoh, Swee-Hin; Goh, Bee Tin; Xu, Chenjie

2016

Gao, Y., Lim, J., Yeo, D. C. L., Liao, S., Lans, M., Wang, Y., et al. (2016). A Selective and Purification-Free Strategy for Labeling Adherent Cells with Inorganic Nanoparticles. ACS Applied Materials & Interfaces, 8(10), 6336-6343.

https://hdl.handle.net/10356/83591

https://doi.org/10.1021/acsami.5b12409

A Selective and Purification-free Strategy for Labeling Adherent Cell with Inorganic Nanoparticles

Yu Gao[a,b], Jing Lim[a], David Yeo[a], Shanshan Liao[a], Malin Lans[a], Yaqi Wang[c], Swee-Hin Teoh[a], Bee Tin Goh[d], Chenjie Xu[a,e*]

[a] School of Chemical and Biomedical Engineering, Nanyang Technological University, 70 Nanyang Drive, Singapore 637457

[b] Key Laboratory for Organic Electronics & Information Displays (KLOEID), Institute of Advanced Materials (IAM), National Synergistic Innovation Center for Advanced Materials (SICAM), Nanjing University of Posts & Telecommunications, 9 Wenyuan Road, Nanjing 210023, China

[c] Hybrid Silica Technologies, Cambridge, MA USA 02139

[d] National Dental Centre of Singapore, Second Hospital Avenue, Singapore 168938

[e] NTU-Northwestern Institute of Nanomedicine, Nanyang Technological University, 50 Nanyang Avenue, Singapore 639798

* Corresponding to cjxu@ntu.edu.sg

Abstract

Cellular labeling with inorganic nanoparticles such as magnetic iron oxide nanoparticles, quantum dots, and fluorescent silica nanoparticles is an important method for the non-invasive visualization of cells using various imaging modalities. Currently, this is mainly achieved through the incubation of cultured cells with the nanoparticles that eventually reach the intracellular compartment through specific or non-specific internalization. This classic method is advantageous in terms of simplicity and convenience, but suffers from issues such as difficulties in fully removing free nanoparticles (suspended in solution) and the lack of selectivity on cell types. This article reports an innovative strategy for the specific labeling of adherent cells without the concern of freely suspended nanoparticles. This method relies on a nanocomposite film which is prepared by homogenously dispersing nanoparticles within a biodegradable polymeric film. When adherent cells are seeded on the film, they adhere, spread, and filtrate into the film through the micropores formed during the film fabrication. The pre-embedded nanoparticles are thus internalized by the cells during this infiltration process. As an example, fluorescent silica nanoparticles were homogenously distributed within a polycaprolactone film by utilizing cryomilling and heat pressing. Upon incubation within physiological buffer, no silica nanoparticles were released from the nanocomposite film even after 20 days incubation. However, when adherent cells (e.g. human mesenchymal stem cells) were grown on the film, they became fluorescent after 3 days, which suggests internalization of silica nanoparticles by cells. In comparison, the suspension cells (e.g. monocytes) in the medium remained non-fluorescent no matter whether there was the presence of adherent cells or not. This strategy eventually allowed the selective and concomitant labelling of mesenchymal stem cells during their harvest from bone marrow aspiration.

Keywords: Selective cell labeling, nanoparticles, nanocomposite polymeric film, adherent cells, mesenchymal stem cells, and bone marrow aspiration

Introduction

Labeling cells with inorganic nanoparticles such as magnetic iron oxide nanoparticles, quantum dots, and fluorescent silica nanoparticles allows non-invasive visualization of cells using various imaging modalities in biomedical research.[1-4] For example, beta cells could be labeled with magnetic nanoparticles and tracked by magnetic resonance imaging to reveal their biodistribution post transplantation.[5] Gold nanoparticles were used to label T-cells and human mesenchymal stem cells (hMSCs), and longitudinally and quantitatively tracked by x-ray computed tomography *in vivo* for cancer immunotherapy and neuropsychiatric disorders respectively.[6, 7] Fluorescent silica nanoparticles were able to label hMCS and to track their tumor homing *in vivo*.[8]

Traditionally, cells are mainly labeled through the simple co-incubation of cells and nanoparticles, in which nanoparticles are internalized through phagocytosis or endocytosis.[9] Transfection agents such as cell penetrating peptide and cationic liposomes, targeting moieties like antibodies, and external stimuli like magnetic field and ultrasound can also be used to facilitate this process.[10-13] In comparison with other methods like electroporation, sonoporation, and microinjection, the co-incubation method is simple, convenient, and cost-effective while limited by the lack of selectivity and the interference of free nanoparticles.[14-16]

This report describes a new method to label cells with nanoparticles. Unlike the co-incubation method, this strategy selectively labels adherent cells without remnant of freely suspended nanoparticles following the cell labelling process. Specifically, the nanoparticles (e.g. silica nanoparticles) were homogenously pre-embedded in a biodegradable polymeric film (e.g. polycaprolactone (PCL)) through cryomilling and heat pressing. The percentage of nanoparticles was controlled at 1% (w/w) and thus the mechanical properties of the nanocomposite film did not change with nanoparticle addition. Although containing micro-sized pores on the surface, the film did not release the nanoparticle component into the solution. However, when adherent cells were seeded on the nanocomposite film, they gradually became fluorescent, suggesting the successful labeling of cells with nanoparticles. In contrast, non-adherent cells seeded into the culture remained unlabelled as a pure population or as a mixed population with adherent cells. This nanoparticle uptake by adherent cells was found to be energy-dependent with phagocytosis being the major mechanism. Finally, unlike conventional cell labelling which adds labelling agents in solution, no free particles were found in the culture medium, which simplifies the purification process.

Results

Fabrication and characterization of nanoparticle doped PCL nanocomposite film

The silica nanoparticles doped nanocomposite film (SiNP-PCL) was fabricated through cryomilling and heat pressing.[17] Briefly, fine powdered PCL particles (median size of ~250 µm) and 200 nm fluorescent silica nanoparticles with the mass ratio of 100:1 were mixed by cryomilling and thermally pressed into the film with a thickness of approximately 30 to 40 µm. While the plain PCL film was semi-transparent and colorless (Figure 1a, c), the SiNP-PCL film was opaque and pink due to the presence of silica nanoparticles (Figure 1b, d). When being visualized under a fluorescence microscope, plain PCL remained non-fluorescent (Figure 1e). On the other hand, the SiNP-PCL film was fluorescent (Figure 1f), suggesting the successful integration and homogenous distribution of silica nanoparticles throughout the PCL film.

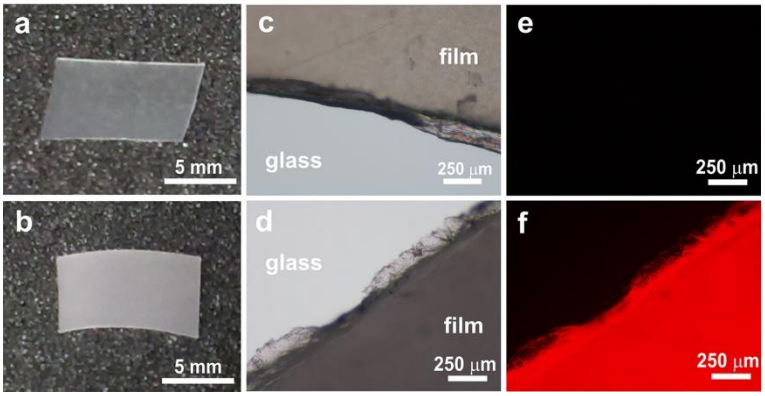

Figure 1. Plain PCL film and SiNP-PCL nanocomposite film: (**a**) Picture of plain PCL film and (**b**) SiNP-PCL nanocomposite film; (**c**, **d**) Bright field and (**e**, **f**) fluorescence images of plain PCL film (**c, e**) and SiNP-PCL nanocomposite film (**d, f**).

Next, the morphology of PCL films was examined with scanning electron microscopy (SEM). As shown in Figure 2a, b, plain PCL film was smooth and presented a continuous surface. However, when silica nanoparticles were present, micron-sized pores appeared on the surface (Figure 2c, d) and within the SiNP-PCL film (cross-section images, Figure S1 in supporting information). In some pores, nanoparticles were observable (Figure 2d). There have been reports to fabricate porous PCL films through porogen leaching.[18] However, in this work, the formation of these microsized pores could come from the evaporation of ice particles, which were generated by the condensation of moisture around hydrophilic silica nanoparticles during the cryomilling.

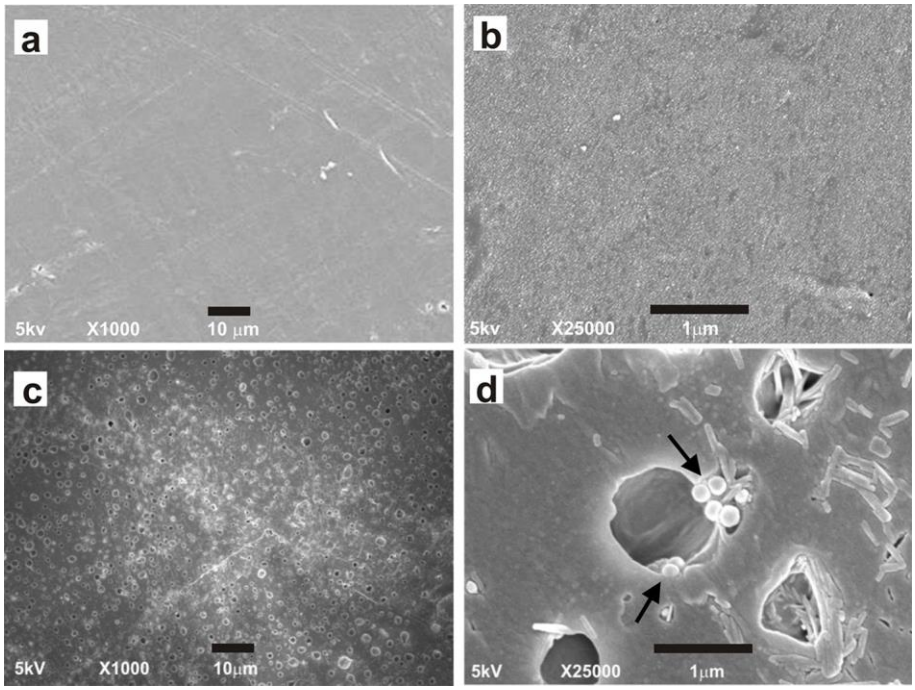

Figure 2. SEM images of the plain PCL film and SiNP-PCL nanocomposite film: (**a**, **b**) plain PCL film and (**c**, **d**) SiNP-PCL nanocomposite film visualized under different resolutions. Scale bars: 10 μm for a and c; 1 μm for b and d. Black arrows indicate the silica nanoparticles.

It is well known that nanoparticle ingredients play a significant role in modulating the mechanical properties of nanocomposite films.[17, 19] Accordingly, the mechanical properties of the films ultimately influence their applications. As such, the mechanical properties of plain PCL and SiNP-PCL films were examined (Table 1). Although the presence of silica nanoparticles resulted in the pores on the film (Figure 2c), these pores did not significantly change the stress-strain curve profile Figure S2 in supporting information) with similar yield strength (13.9 ± 1.2 MPa) and Young's modulus (195.7 ± 39.1 MPa) to plain PCL film (10.8 ± 1.9 MPa for yield strength and 192.9 ± 38.4 MPa for Young's modulus). This should be attributed to the low percentage of nanoparticles (1% w/w) in the composite. However, there was a slight increase of the toughness from 4.5 ± 0.7 to 8.3 ± 2.1 MJm^{-3} after the incorporation of silica nanoparticles. This is due to the reinforcement effect of silica nanoparticles, which has been reported in $CaCO_3$ nanoparticles doped PCL film.[20]

Table 1. Mechanical properties of the plain PCL film and SiNP-PCL nanocomposite film

Composition	Yield strength (MPa)	Young's Modulus (MPa)	Toughness (MJm^{-3})
PCL	10.8 ± 1.9	192.9 ± 38.4	4.5 ± 0.7
SiNP-PCL	13.9 ± 1.2	195.8 ± 39.1	8.3 ± 2.1

Labeling of adherent cells with SiNP-PCL nanocomposite film

hMSCs are the major stem cells for cell therapy.[21-23] Nanoparticle labeling would allow them to be tracked in preclinical or clinical models for revealing their biodistribution.[24, 25] Here they were seeded on the SiNP-PCL film and collected through trypsinization at day 3, 5, and 7. The collected hMSCs were stained with DAPI (blue, for nucleus) and DiO (green, for membrane) before being placed on cover slides and imaged by fluorescence microscope. As shown in Figure 3a, the originally non-fluorescent hMSCs became fluorescent from day 3, when 15% hMSCs were labeled with fluorescent silica nanoparticles. As time went on, a greater proportion of cells became labeled. Fluorescent cells were 82% and 99% of the whole population at day 5 and 7 subsequently (Figure 3b). Under confocal scanning microscopy, nanoparticles were found to reside in the cytoplasm of cells (Figure 3c).

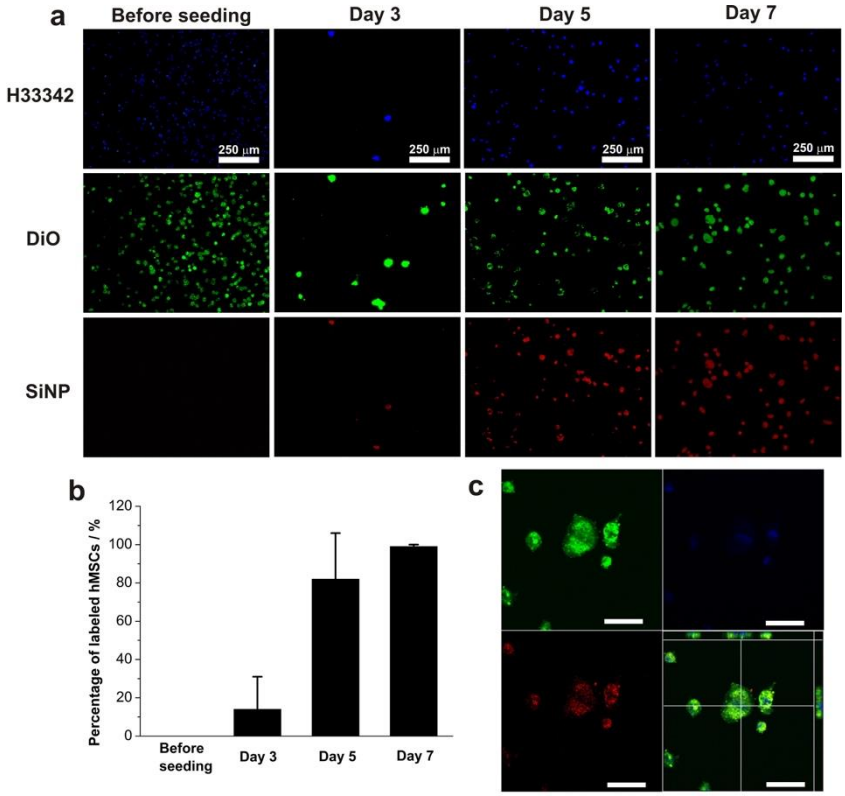

Figure 3. hMSCs before seeding and hMSCs cultured on the SiNP-PCL nanocomposite film for 3, 5 and 7 days: (**a**) Representative fluorescence images of hMSCs before seeding and hMSCs cultured on the SiNP-PCL nanocomposite film at day 3, 5 and 7. Hoechst 33342 stains the nucleus (blue), DiO stains the membrane (green), and red color represents silica nanoparticles. (**b**) Quantification of fluorescent silica nanoparticle labeled hMSCs before and after 3, 5, and 7 days labeling. (**c**) Confocal scanning microscopy of hMSCs cultured on SiNP-PCL film for 3 days. Scale bar: 50 μm.

Although the adherent cells cultured on the film could be labeled with nanoparticles that were pre-embedded in the PCL film, interestingly, there was no free silica nanoparticles released into the solution (Figure S3a, b in supporting information). Even when the nanocomposite film was processed with NaOH solution for 24 hours to accelerate the

degradation of PCL,[26] minimal fluorescence (indicative of silica nanoparticles) in the solution was observed during an incubation period of 20 days (Figure 4a). However, the NaOH processing did improve the fluorescence intensity of cells while the other conditions were kept the same (Figure 4b). This indicates that the cell labeling on SiNP-PCL film is related with the degradation of PCL.

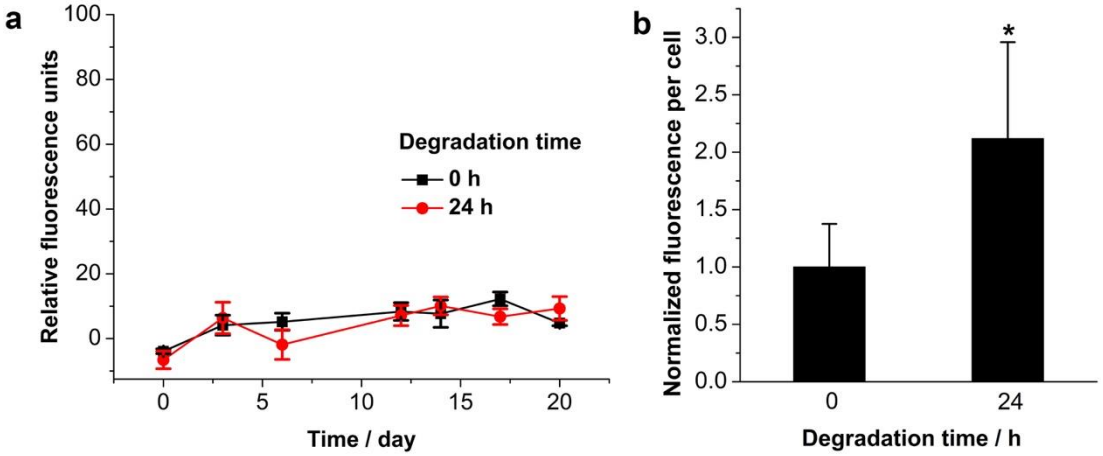

Figure 4. The influence of NaOH treatment over the SiNP-PCL nanocomposite film: (**a**) Silica nanoparticle release profile from SiNP-PCL composite film that was pre-treated with 3M NaOH for 0 or 24 hours. (**b**) Normalized fluorescence intensity per cell after 7 days culturing on SiNP-PCL nanocomposite film that was pre-treated with 3M NaOH for 0 or 24 hours. The fluorescence per cell was calculated by measurement of the intensity (red) per cell by ImageJ. * denotes $p < 0.05$.

After the successful labeling of hMSCs, we next set to examine whether this phenomenon was universal to other adherent cells. Thus another type of adherent cells, human colorectal carcinoma cells (RKO) were then seeded on the SiNP-PCL film. As expected, RKO cells became fluorescent when being cultured on the SiNP-PCL films (Figure S4a in supporting information) and the labeling speed was even faster than that of hMSCs. At day 3, only 15% hMSCs were labeled with silica nanoparticles while 94% RKO were labeled (Figure S4b in supporting information).

Selective labeling of adherent cells

Besides adherent cells, suspension cells including human promyelocytic leukemia cells (HL60) and leukemic monocyte lymphoma cells (U937) were also tested by being seeded in the well containing the SiNP-PCL film for 3, 5 and 7 days. During the 7 day culturing, both HL60 (Figure 5) and U937 cells (Figure S5 in supporting information) remained non-

fluorescent. These suspension cells only became labeled when free silica nanoparticles were added in solution.

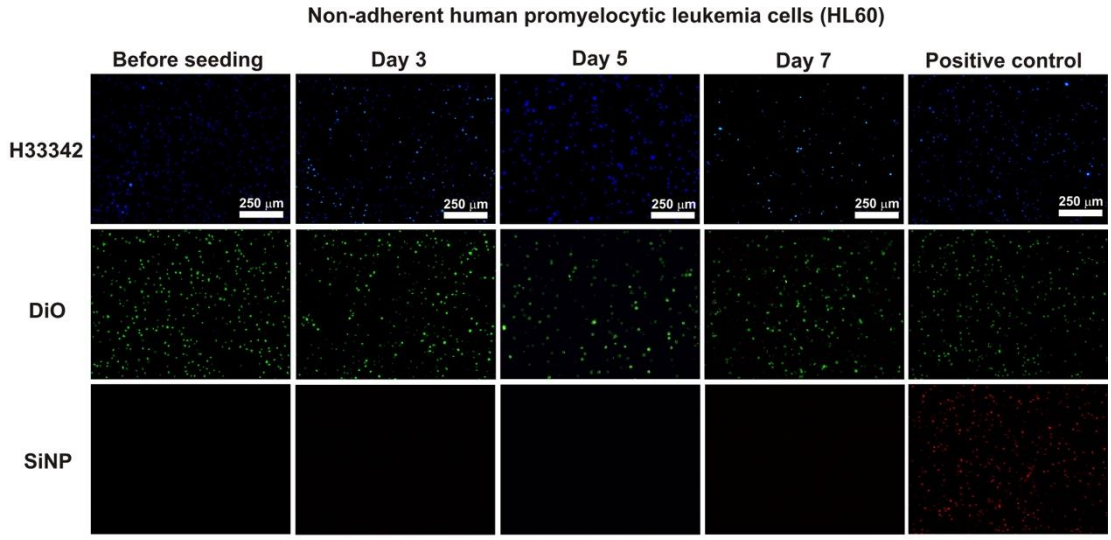

Figure 5. Representative fluorescence images of HL60 cells before seeding and HL60 cells seeded in the well containing SiNP-PCL nanocomposite film for 3, 5 and 7 days. Positive control represents cells seeded in the solution containing 4 μg/mL free silica nanoparticles. Hoechst 33342 stains the nuclear (blue), DiO stains the membrane (green), and red color represents silica nanoparticles.

The inability of suspension cells to uptake SiNPs from the SiNP-PCL film presents a strategy for the selective labeling of adherent cells. To test this hypothesis, the adherent cells (i.e. RKO cells, stained in green) and suspension cells (i.e. U937 cells, stained in blue) were co-cultured in the well containing the SiNP-PCL film for 3 days. As shown in Figure 6a, only the adherent cells were successfully labeled with silica nanoparticles (red). The non-adherent U937 cells failed to show any detectable fluorescence signal from silica nanoparticles (Figure 6b).

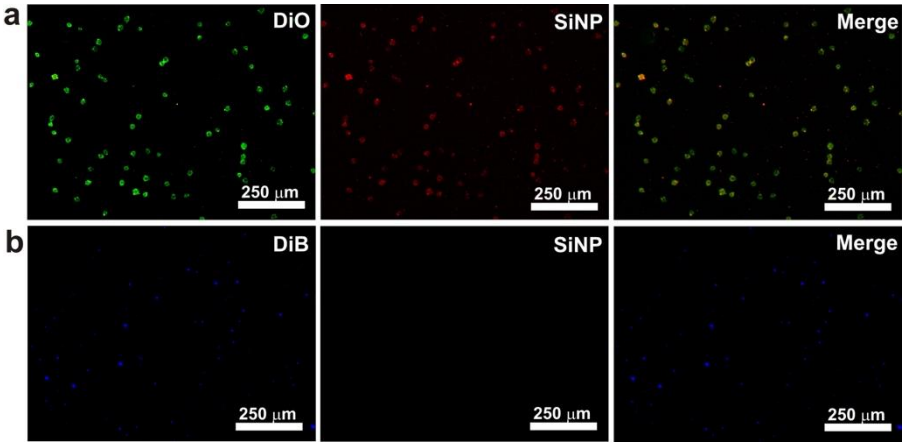

Figure 6. Selective labeling of adherent RKO cells in the mixture of RKO cells and U937 cells by SiNP-PCL nanocomposite film during a 3 day culturing: (**a**) RKO cells originally

stained in green were labeled with silica nanoparticles (red). (**b**) Non-adherent U937 cells originally stained in blue were not labeled with silica nanoparticles.

Mechanism for the labeling of adherent cells by SiNP-PCL nanocomposite film

Inhibitors targeting various kinds of endocytosis pathway were chosen to block the cell labeling by silica nanoparticles.[12, 27] Specifically, the mixture of sodium azide and 2-deoxy-D-glucose blocks the production of ATP and consequently the energy dependent cellular uptake. Chlorpromazine and genistein inhibit clathrin-mediated and caveolae-mediated endocytosis respectively, while amiloride blocks macropinocytosis and cytochalasin D targets phagocytosis. During the experiment, adherent RKO cells were seeded on the SiNP-PCL film for 1 hour to allow the attachment. Then inhibitors were added to the medium and incubated for 24 hours. After being rinsed with PBS, cells were collected from the SiNP-PCL film for imaging. As shown in Figure 7, treatment with sodium azide and 2-deoxy-D-glucose (shortened as sodium azide) reduced the average fluorescence per cell by ~63.4% in comparison to control group (no inhibitor). The decrease of cellular fluorescence was clearly due to the reduced transfer of silica nanoparticles from the film to the cells. Thus the cell labeling with SiNP-PCL film was energy-dependent. Cytochalasin D had the next most potent effect on inhibiting cell labeling, decreasing cellular fluorescence by 60.7%. This indicated that phagocytosis was mainly responsible for the nanoparticle uptake from the nanocomposite film. When chlorpromazine and genistein were used, the cellular fluorescence was reduced by 23.3% and 22.7% respectively, which indicated that clathrin- and caveolae-mediated endocytosis were partially responsible for the nanoparticle uptake. Macropinocytosis may also be involved in the uptake process given that amiloride reduced 33.8% of the cellular fluorescence.

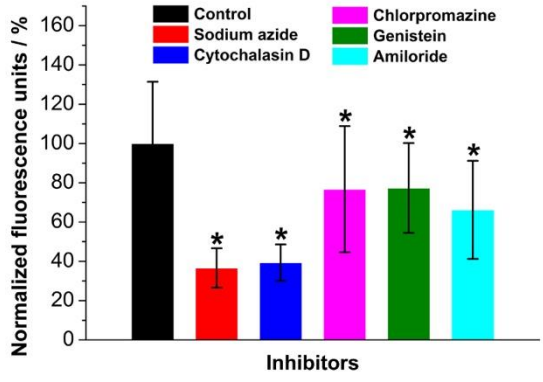

Figure 7. Inhibition of RKO cell labeling by SiNP-PCL nanocomposite film by different endocytosis inhibitors. Under each condition, at least 150 cells were analyzed. * denotes $p < 0.05$.

Selective and concomitant labeling of rabbit MSCs during their harvest from bone marrow aspiration

Finally, SiNP-PCL nanocomposite film was used to selectively label MSCs in the bone marrow aspiration during the harvest. Harvest of MSCs from bone marrow relies on the plastic adherent nature of MSCs, which is not possessed by the other cell types in the bone marrow such as red blood cells and haematopoetic progenitors. Specifically, freshly extracted rabbit bone marrow aspirate was diluted and washed by medium, and then was directly seeded on 24 well plates covered with SiNP-PCL nanocomposite film or not (Figure 8a and Figure S6 in supporting information). After 15 days culturing, other cell components were removed (during the routine medium change, as they do not attach on the film) while MSCs were collected from the surface of nanocomposite film through trypsinization for imaging. As shown in Figure 8b, c, rabbit MSCs collected from normal culture plate did not exhibit any SiNP signal. In contrast, MSCs collected from the SiNP-PCL nanocomposite film showed the fluorescence signal of SiNPs, suggesting the successful SiNP uptake/labeling (Figure 8c). Osteogenetic and adipogenetic differentiation assay of collected cells were performed that further confirmed the multipotency of MSCs (Figure S7 in supporting information).

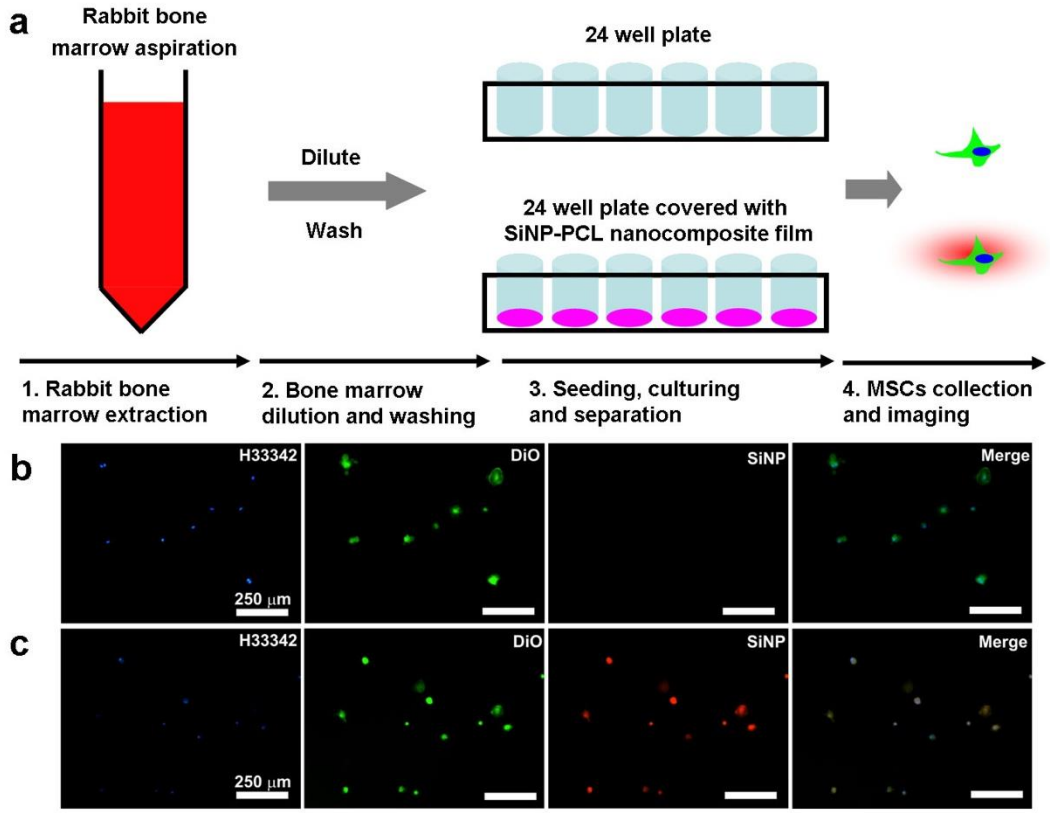

Figure 8. Selective labeling of rabbit MSCs from rabbit bone marrow aspiration during their harvest: (**a**) Schematic illustration of rabbit MSCs harvest and labeling from freshly extracted bone marrow aspirate by directly seeding on SiNP-PCL nanocomposite film. (**b**) Fluorescence imaging of collected MSCs from normal 24 well plate after 15 days culturing. (**c**) Fluorescence imaging of collected MSCs from 24 well plate covered with SiNP-PCL nanocomposite film after 15 days culturing.

Discussion

Nanocomposite films hold great promise in emerging biomedical applications such as tissue engineered scaffold,[19, 28-30] implanted drug delivery platform,[31, 32] and antibacterial packaging.[33-35] This work reports a novel application of nanocomposite films, i.e. the selective labeling of adherent cells with nanoparticles that are pre-embedded in the film.

As a proof-of-concept, silica nanoparticles were embedded within the 30-40 μm thick PCL film through cryomilling and heat pressing. The weight percentage of silica nanoparticles was 1% to minimize changes to the mechanical properties of the PCL film. Similar yield strength and Young's modulus were found between plain PCL and SiNP-PCL nanocomposite films, with an increased toughness for SiNP-PCL caused by the reinforcement effect of the doped silica nanoparticles. Due to the presence of silica nanoparticles, the nanocomposite film was fluorescent and contained micron-sized pores that might be a result of ice particle evaporation. The embedded silica nanoparticles were not readily released from the film into the solution, even when the film degradation was accelerated by exposure to NaOH.

When adherent cells such as hMSCs and RKO cells were seeded on the film, they spread on the surface, infiltrated into the micron-pores,[36] and interacted closely with the silica nanoparticles. Through phagocytosis, the cells took up the silica nanoparticles and become labeled. Labeling of RKO cells was found to be more efficient than that of hMSCs. This difference is likely to be attributed to the differences of phagocytosis capabilities and uptake kinetics between different cell lines.[37] Theoretically, if the difference of phagocytosis activities is significant enough while ignoring the proliferation rate of two kinds of adherent cells, this method can selective label the adherent cells with higher phagocytosis activity. In contrast, non-adherent cells such as HL60 and U937 cells were not labeled during the incubation with the nanocomposite film, because they lack the ability to infiltrate the nanocomposite films unlike the adherent cells.[38, 39]

A potential application of this SiNP-PCL composite film is to selectively label adherent cells in a cell mixture composed of multiple cell types. As a proof of concept, adherent RKO and non-adherent U937 cells were mixed and co-cultured in a well containing SiNP-PCL film. The fluorescence of silica nanoparticles was only observed within RKO cells, suggesting the successful labeling of adherent cells with good selectivity.

This selective labeling of adherent cells by the nanoparticles pre-embedded within the nanocomposite film will be attractive for researchers in regenerative medicine and cancer research. Currently, a typical stem cell transplantation experiment consists of three steps

including cell isolation and purification, cell labeling and transplantation, and subsequent imaging for monitoring safety and efficacy.[4] Taking hMSCs as an example, their harvest from human bone marrow relies on the plastic adherent nature of hMSCs, which is not possessed by the other cell types in the bone marrow such as red blood cells and haematopoetic progenitors.[40] In the present work, the rabbit bone marrow aspiration was plated directly on the nanoparticle-embedded nanocomposite film, rabbit MSCs were found to be labeled with nanoparticles during the harvesting and isolation, without the need of further labeling. This is especially promising for tracking therapeutic hMSCs because it provides a simple method to label cells during their isolation and expansion. In cancer research, tracking circulating tumor cells (CTC) during metastasis progression is essential for the understanding of the mechanism of metastasis cancer.[41, 42] Another potential application of this technology is to selectively label the CTCs that are undergoing mesenchymal-epithelial transition (MET) that is critical for tumor metastasis.

Conclusion

In summary, silica nanoparticles doped PCL nanocomposite film was fabricated through cryomilling and heat pressing. The use of cryomilling allowed the homogenous distribution of silica nanoparticles throughout the film. Although silica nanoparticles were not released from the nanocomposite film into solution during the incubation, adherent cells grown on the film were able to actively uptake the nanoparticles through phagocytosis. As this phenomenon was specific for adherent cells, it provides a strategy to selectively label adherent cells with nanoparticles, which has great potential in the fields of regenerative medicine and cancer therapy.

Methods

All chemicals except specifically mentioned were purchased from Sigma-Aldrich. Fluorescent silica nanoparticles (C spec®, TRITC, 200 nm of diameter) with surface coatings of polyethylenimine were provided by Hybrid Silica Technologies, MA, USA.

Synthesis of silica nanoparticle doped PCL film. Medical grade PCL pellets (> 500 μm) (Osteopore International, Singapore) were weighed and placed into a stainless steel jar, before they were pulverized in a cryomilling process (Retsch®, Germany) at low temperature cooled by liquid nitrogen. Then silica nanoparticles and cryomilled PCL (mass ratio of 1:100) were mixed and cryomilled again for 20 minutes to attain powdered SiNP-PCL. The powders were then thermally pressed into a thin film (30 to 40 μm) between two stainless steel sheets at 80 °C (Carver Inc, USA). The film was then stored in a dry cabinet (Digi-Cabi AD-100, Singapore) before use.

Scanning electron microscopy. Small piece (5×5 mm^2) of plain PCL or SiNP-PCL nanocomposite film was first coated with 10 nm platinum to increase their conductivity, and then imaged by field emission scanning electron microscopy (JEOL-JSM-7600F).

Mechanical characterization. SiNP-PCL nanocomposite film or plain PCL film was tested by an Instron tester (Instron 5582, USA). The films were first cut into rectangular cross-sections 10 mm in width and 30 mm in gauge length. They were then secured onto paper frames to minimize slippage during the test. A cross-head moving speed of 3 mm/min (10% of gauge length) was applied, and the corresponding tensile force and extension were recorded. The yield strength, strain, and Young's moduli were reported. The results were the average of 6 samples.

Nanoparticle release characterization. SiNP-PCL composite films were evaluated for their release characteristics. Briefly, the films were cut with equal areas (equal masses), placed in 24 well plates and immersed in 1 mL of phosphate buffer saline (PBS) under constant, gentle agitation. At different time points, the solutions of each well were removed for fluorescence (excitation at 550 nm, emission at 570 nm) reading (Spectramax M5, USA). Another 1 mL of PBS was replenished into each well after removal. Triplicates of each sample were performed.

To accelerate the degradation of SiNP-PCL composite film, the films were soaked into 3 mol/L of NaOH solution for 24 hours. After washing with PBS, they were placed into the 24 well plate for either cell labelling assay or nanoparticle release measurement.

Cell culture. Adherent cells including human mesenchymal stem cells (hMSCs) and human colorectal carcinoma cells (RKO) were purchased from Lonza (USA) and ATCC (USA) respectively. hMSCs were cultured in mesenchymal stem cell growth medium (Lonza) and RKO were cultured in Dulbecco's modified eagle medium (DMEM, Gibco) supplemented with 10% fetal bovine serum (FBS, Gibco) and 1% penicillin-streptomycin (Gibco). They were placed in an incubator at 37 °C with 5% CO_2, and routine sub-culture was performed every 3 to 7 days. Non-adherent cells including human promyelocytic leukemia cells (HL60) and leukemic monocyte lymphoma cells (U937) were purchased from HyClone (USA), and cultured in RPMI 1640 medium (HyClone) with 10% FBS. They were sub-cultured every 2 to 3 days.

Cell labeling with SiNP-PCL nanocomposite film. The film was cut into round pieces (12 mm in diameter) and then glued onto 12 mm coverslips. The whole compartment was sterilized by immersing into 100% ethanol for 24 hours. After washing with PBS for more than three times, the films were placed into a 24 well plate and pre-incubated with 0.5 mL cell medium for 1 hour before seeding. All cells were seeded at the density of 2×10^4 per well and incubated at 37 °C with 5% CO_2. The cells were examined at day 1, 2, and 3 for RKO, and at

day 3, 5, 7 for hMSCs, HL60, and U937 with an inverted fluorescent microscope (LX71, Olympus).

Cells were collected at different time points and washed by PBS twice. Then the cells were re-suspended in DMEM medium supplemented with 1 μg/mL Hoechst 33342 and 5 μg/mL Vybrant DiO membrane dye (Invitrogen). The cell suspension was incubated on ice for 15 minutes before cells were collected, washed with PBS. For adherent cells (hMSCs and RKO), they were added onto a cover slide pre-coated with fibronectin (Lonza) and then incubated at 37 °C for 5 minutes, followed by cell fixation and fluorescence imaging. For non-adherent cells, they were added to a 35 mm imaging dish (ibidi, Germany). All the cells were imaged by an inverted microscope (LX71, Olympus). To quantify the percentage of labelled cells, an intensity threshold of the red colour was set based on the intensity of the control group. Then the cells whose intensity higher than the threshold were counted as labelled cells. At least 200 cells were analyzed for each group.

Confocal laser scanning microscopy. hMSCs cultured on the SiNP-PCL nanocomposite film were washed with PBS for 3 times. Then cells were collected through trypsinization and re-suspended in DMEM supplemented with 1 μg/mL Hoechst 33342 and 5 μg/mL Vybrant DiO membrane dye. The cell suspension was incubated on ice for 15 minutes before cells were collected, washed with PBS, and added onto a cover slide pre-coated with fibronectin. After staying at cell incubator for 5 minutes, the cells were fixed and imaged by a Zeiss LSM710 META confocal microscope.

Nanoparticle uptake mechanism. RKO cancer cells were first seeded on the SiNP-PCL nanocomposite film and incubate for 1 hour to allow the attachment. Then solutions of different inhibitors were added to achieve 10 mM sodium azide and 20 mM 2-deoxy-D-glucose, 10 μg/ml chlorpromazine, 200 μM genistein, 50 μg/ml amiloride, or 5 μg/ml cytochalasin D respectively. After 24 hours, cells were rinsed with PBS for three times, collected through trypsinization, and re-seeded on a fibronectin coated culture plate and supplemented with full medium. Cells were incubated for another 2 hours for attachment before the fluorescence imaging. For signal quantification, the fluorescence intensity of each group (at least 150 cells per sample) was quantified through ImageJ. The statistical significance was determined by calculating the p value using Student's t-test (two-tailed distribution and two-sample unequal variance).

Rabbit bone marrow harvesting. All procedures involving animals were approved by the Institutional Animal Care and Use Committee (IACUC) of Singapore. Two healthy adult male, New Zealand white rabbits, with an age of 2 months and weight of 2-2.5 kg were used for bone marrow aspiration in this study. The procedure was performed under general

anaesthesia. The right iliac crest region of the rabbits was cleansed with iodine and alcohol. The harvesting of bone marrow was performed percutaneously under sterile conditions. The bone marrow aspiration needle was connected to a 10 ml plastic syringe which was rinsed with 1 ml of heparin (5,000 units per ml). The needle was then punctured into the right iliac crest and about 5 ml of bone marrow was aspirated. The bone marrow aspirate was transferred into a 10 ml tube which was then kept in ice.

Rabbit MSC separation and labelling on SiNP-PCL nanocomposite film. Freshly extracted rabbit bone marrow aspirate was first diluted for 10 times by DMEM. Then the diluted solution was washed by DMEM for at least three times, and was directly seeded on 24 well plate covered with SiNP-PCL nanocomposite film. The cells were kept in incubator and routine medium change was perfumed every three days. After 15 days culturing, attached MSCs were collected through trypsinization from 24 well plate or SiNP-PCL nanocomposite film, and then were re-seeded in new culture plates. MSCs were stained by H33342 and DiO as mentioned above and imaged by inverted microscope.

ASSOCIATED CONTENT

Supporting Information. SEM images of the cross-section of SiNP-PCL nanocomposite film with different resolutions, stress-strain curves of PCL and SiNP-PCL nanocomposite films, Silica nanoparticle release profile of SiNP-PCL nanocomposite film, RKO cell labeling with SiNP-PCL nanocomposite film, non-adherent U937 labeling when cultured on SiNP-PCL nanocomposite film, rabbit bone marrow extraction procedure, osteogenic and adipogenic differentiation assay of collected cells from rabbit bone marrow aspirate that seeded on SiNP-PCL nanocomposite film.

This material is available free of charge via the Internet at http://pubs.acs.org.

Author Contributions

The manuscript was written through contributions of all authors. All authors have given approval to the final version of the manuscript. Specifically, Y.G. and C.J.X. conceived the project and wrote the manuscript. Y.G., J.L, D.Y., S.L, and M.L performed the experiments. Y.Q, S.H.T, and B.T.G helped plan the experiments and provided valuable input during the manuscript preparation.

Notes

The authors declare no conflict of interest.

ACKNOWLEDGEMENTS

The work was supported by the Tier-1 Academic Research Funds by Singapore Ministry of Education (RG64/12 to XCJ; RGT21/13 to TSH) and NTU-NU Institute of Nanomedicine (M4081502.F40 to X.C.J).

REFERENCES

1. Naumova, A. V.; Modo, M.; Moore, A.; Murry, C. E.; Frank, J. A. Clinical Imaging in Regenerative Medicine. *Nat. Biotechnol.* **2014**, 32, 804-818.

2. Gao, Y.; Lim, J.; Teoh, S. H.; Xu, C. Emerging Translational Research on Magnetic Nanoparticles for Regenerative Medicine. *Chem. Soc. Rev.***2015**, 44, 6306-6329

3. Gao, Y.; Cui, Y.; Chan, J. K.; Xu, C. Stem Cell Tracking with Optically Active Nanoparticles. *Am. J. Nucl. Med. Mol. Imaging* **2013**, 3, 232-246.

4. Nguyen, P. K.; Riegler, J.; Wu, J. C. Stem Cell Imaging: From Bench to Bedside. *Cell Stem Cell* **2014**, 14, 431-444.

5. Evgenov, N. V.; Medarova, Z.; Dai, G.; Bonner-Weir, S.; Moore, A. In Vivo Imaging of Islet Transplantation. *Nat. Med.* **2006**, 12, 144-148.

6. Meir, R.; Shamalov, K.; Betzer, O.; Motiei, M.; Horovitz-Fried, M.; Yehuda, R.; Popovtzer, A.; Popovtzer, R.; Cohen, C. J. Nanomedicine for Cancer Immunotherapy: Tracking Cancer-Specific T-Cells in Vivo with Gold Nanoparticles and CT Imaging. *ACS Nano* **2015**, 9, 6363-6372.

7. Betzer, O.; Shwartz, A.; Motiei, M.; Kazimirsky, G.; Gispan, I.; Damti, E.; Brodie, C.; Yadid, G.; Popovtzer, R. Nanoparticle-Based CT Imaging Technique for Longitudinal and Quantitative Stem Cell Tracking within the Brain: Application in Neuropsychiatric Disorders. *ACS Nano* **2014**, 8, 9274-9285.

8. Gao, Y.; Wang, Y.; Fu, A.; Shi, W.; Yeo, D.; Luo, K. Q.; Ow, H.; Xu, C. Tracking Mesenchymal Stem Cell Tumor-homing Using Fluorescent Silica Nanoparticles. *J. Mater. Chem. B* **2015**, 3, 1245-1253.

9. Zhao, F.; Zhao, Y.; Liu, Y.; Chang, X.; Chen, C.; Zhao, Y. Cellular Uptake, Intracellular Trafficking, and Cytotoxicity of Nanomaterials. *Small* **2011**, 7, 1322-1337.

10. Copolovici, D. M.; Langel, K.; Eriste, E.; Langel, Ü. Cell-Penetrating Peptides: Design, Synthesis, and Applications. *ACS Nano* **2014**, 8, 1972-1994.

11. Kito, T.; Shibata, R.; Ishii, M.; Suzuki, H.; Himeno, T.; Kataoka, Y.; Yamamura, Y.; Yamamoto, T.; Nishio, N.; Ito, S.; Numaguchi, Y.; Tanigawa, T.; Yamashita, J. K.; Ouchi, N.; Honda, H.; Isobe, K.; Murohara, T. iPS Cell Sheets Created by a Novel Magnetite Tissue Engineering Method for Reparative Angiogenesis. *Sci. Rep.* **2013**, 3, 1418

12. Gao, H.; Yang, Z.; Zhang, S.; Cao, S.; Shen, S.; Pang, Z.; Jiang, X. Ligand Modified Nanoparticles Increases Cell Uptake, Alters Endocytosis and Elevates Glioma Distribution and Internalization. *Sci. Rep.* **2013**, 3, 2534

13. Mura, S.; Nicolas, J.; Couvreur, P. Stimuli-responsive Nanocarriers for Drug Delivery. *Nat. Mater.* **2013**, 12, 991-1003.

14. Mellott, A.; Forrest, M. L.; Detamore, M. Physical Non-Viral Gene Delivery Methods for Tissue Engineering. *Ann. Biomed. Eng.* **2013**, 41, 446-468.

15. Lentacker, I.; De Cock, I.; Deckers, R.; De Smedt, S. C.; Moonen, C. T. W. Understanding Ultrasound Induced Sonoporation: Definitions and Underlying Mechanisms. *Adv. Drug Delivery Rev.* **2014**, 72, 49-64.

16. Yeo, D. C.; Wiraja, C.; Zhou, Y.; Tay, H. M.; Xu, C.; Hou, H. W. Interference-free Micro/nanoparticle Cell Engineering by Use of High-Throughput Microfluidic Separation. *ACS Appl. Mater. Interfaces* **2015**, 7, 20855-20864.

17. Lim, J.; Chong, M. S. K.; Chan, J. K. Y.; Teoh, S. H. Polymer Powder Processing of Cryomilled Polycaprolactone for Solvent-Free Generation of Homogeneous Bioactive Tissue Engineering Scaffolds. *Small* **2014**, 10, 2495-2502.

18. Allaf, R. M.; Rivero, I. V.; Abidi, N.; Ivanov, I. N. Porous Poly(ε-caprolactone) Scaffolds for Load-bearing Tissue Regeneration: Solventless Fabrication and Characterization. *J. Biomed. Mater. Res., Part B* **2013**, 101B, 1050-1060.

19. Yate, L.; Coy, L. E.; Gregurec, D.; Aperador, W.; Moya, S. E.; Wang, G. Nb–C Nanocomposite Films with Enhanced Biocompatibility and Mechanical Properties for Hard-Tissue Implant Applications. *ACS Appl. Mater. Interfaces* **2015**, 7, 6351-6358.

20. Abdolmohammadi, S.; Siyamak, S.; Ibrahim, N. A.; Yunus, W. M. Z. W.; Rahman, M. Z. A.; Azizi, S.; Fatehi, A. Enhancement of Mechanical and Thermal Properties of Polycaprolactone/Chitosan Blend by Calcium Carbonate Nanoparticles. *Int. J. Mol. Sci.* **2012**, 13, 4508-4522.

21. Uccelli, A.; Moretta, L.; Pistoia, V. Mesenchymal Stem Cells in Health and Disease. *Nat. Rev. Immunol.* **2008**, 8, 726-736.

22. Salem, H. K.; Thiemermann, C. Mesenchymal Stromal Cells: Current Understanding and Clinical Status. *Stem Cells* **2010**, 28, 585-596.

23. Bianco, P.; Cao, X.; Frenette, P. S.; Mao, J. J.; Robey, P. G.; Simmons, P. J.; Wang, C. Y. The Meaning, the Sense and the Significance: Translating the Science of Mesenchymal Stem Cells into Medicine. *Nat. Med.* **2013**, 19, 35-42.

24. Xu, C.; Miranda-Nieves, D.; Ankrum, J. A.; Matthiesen, M. E.; Phillips, J. A.; Roes, I.; Wojtkiewicz, G. R.; Juneja, V.; Kultima, J. R.; Zhao, W.; Vemula, P. K.; Lin, C. P.; Nahrendorf, M.; Karp, J. M. Tracking Mesenchymal Stem Cells with Iron Oxide Nanoparticle Loaded Poly(lactide-co-glycolide) Microparticles. *Nano Lett.* **2012**, 12, 4131-4139.

25. Huang, X.; Zhang, F.; Wang, Y.; Sun, X.; Choi, K. Y.; Liu, D.; Choi, J.-s.; Shin, T.-H.; Cheon, J.; Niu, G.; Chen, X. Design Considerations of Iron-Based Nanoclusters for Noninvasive Tracking of Mesenchymal Stem Cell Homing. *ACS Nano* **2014**, 8, 4403-4414.

26. Lee, S.-H.; Lee, J.; Cho, Y.-S. Analysis of Degradation Rate for Dimensionless Surface Area of Well-interconnected PCL Scaffold via In-vitro Accelerated Degradation Experiment. *J. Tissue Eng. Regener. Med.* **2014**, 11, 446-452.

27. Wiraja, C.; Yeo, D. C.; Chew, S. Y.; Xu, C. Molecular Beacon-loaded Polymeric Nanoparticles for Non-invasive Imaging of mRNA Expression. *J. Mater. Chem. B* **2015**, 3, 6148-6156.

28. Tian, H.-C.; Liu, J.-Q.; Wei, D.-X.; Kang, X.-Y.; Zhang, C.; Du, J.-C.; Yang, B.; Chen, X.; Zhu, H.-Y.; NuLi, Y.-N.; Yang, C.-S. Graphene Oxide Doped Conducting Polymer Nanocomposite Film for Electrode-tissue Interface. *Biomaterials* **2014**, 35, 2120-2129.

29. Wang, J. H.; He, C. L.; Cheng, N. M.; Yang, Q.; Chen, M. M.; You, L. J.; Zhang, Q. Q. Bone Marrow Stem Cells Response to Collagen/Single-Wall Carbon Nanotubes-COOHs Nanocomposite Films with Transforming Growth Factor Beta 1. *J. Nanosci. Nanotechnol.* **2015**, 15, 4844-4850.

30. Luo, X. L.; Weaver, C. L.; Tan, S. S.; Cui, X. T. Pure Graphene Oxide Doped Conducting Polymer Nanocomposite for Bio-interfacing. *J. Mater. Chem. B* **2013**, 1, 1340-1348.

31. Weaver, C. L.; LaRosa, J. M.; Luo, X. L.; Cui, X. T. Electrically Controlled Drug Delivery from Graphene Oxide Nanocomposite Films. *ACS Nano* **2014**, 8, 1834-1843.

32. Huang, G. W.; Xiao, H. M.; Fu, S. Y. Electrical Switch for Smart pH Self-Adjusting System Based on Silver Nanowire/Polyaniline Nanocomposite Film. *ACS Nano* **2015**, 9, 3234-3242.

33. Sorrentino, A.; Gorrasi, G.; Vittoria, V. Potential Perspectives of Bio-nanocomposites for Food Packaging Applications. *Trends Food Sci. Technol.* **2007**, 18, 84-95.

34. Kubacka, A.; Serrano, C.; Ferrer, M.; Lunsdorf, H.; Bielecki, P.; Cerrada, M. A. L.; Fernandez-Garcia, M. High-performance Dual-action Polymer-TiO_2 Nanocomposite Films via Melting Processing. *Nano Lett.* **2007**, 7, 2529-2534.

35. Pangule, R. C.; Brooks, S. J.; Dinu, C. Z.; Bale, S. S.; Salmon, S. L.; Zhu, G. Y.; Metzger, D. W.; Kane, R. S.; Dordick, J. S. Antistaphylococcal Nanocomposite Films Based on Enzyme-Nanotube Conjugates. *ACS Nano* **2010**, 4, 3993-4000.

36. Wang, Z.; Teoh, S. H.; Hong, M.; Luo, F.; Teo, E. Y.; Chan, J. K. Y.; Thian, E. S. Dual-Microstructured Porous, Anisotropic Film for Biomimicking of Endothelial Basement Membrane. *ACS Appl. Mater. Interfaces* **2015**, 7, 13445-13456.

37. dos Santos, T.; Varela, J.; Lynch, I.; Salvati, A.; Dawson, K. A. Quantitative Assessment of the Comparative Nanoparticle-Uptake Efficiency of a Range of Cell Lines. *Small* **2011**, 7, 3341-3349.

38. Soh, S.; Kandere-Grzybowska, K.; Mahmud, G.; Huda, S.; Patashinski, A. Z.; Grzybowski, B. A. Tomography and Static-Mechanical Properties of Adherent Cells. *Adv. Mater.* **2012**, 24, 5719-5726.

39. Fischer-Friedrich, E.; Hyman, A. A.; Julicher, F.; Muller, D. J.; Helenius, J. Quantification of Surface Tension and Internal Pressure Generated by Single Mitotic Cells. *Sci. Rep.* **2014**, 4, 6213

40. Prockop, D. J. Marrow Stromal Cells as Stem Cells for Nonhematopoietic Tissues. *Science* **1997**, 276, 71-74.

41. Nedosekin, D. A.; Verkhusha, V. V.; Melerzanov, A. V.; Zharov, V. P.; Galanzha, E. I. In Vivo Photoswitchable Flow Cytometry for Direct Tracking of Single Circulating Tumor Cells. *Chem. Biol.* **2014**, 21, 792-801.

42. Dorsey, J. F.; Kao, G. D.; MacArthur, K. M.; Ju, M.; Steinmetz, D.; Wileyto, E. P.; Simone, C. B.; Hahn, S. M. Tracking Viable Circulating Tumor Cells (CTCs) in

the Peripheral Blood of Non Small Cell Lung Cancer (NSCLC) Patients Undergoing Definitive Radiation Therapy: Pilot Study Results. *Cancer* **2015**, 121, 139-149.

TOC

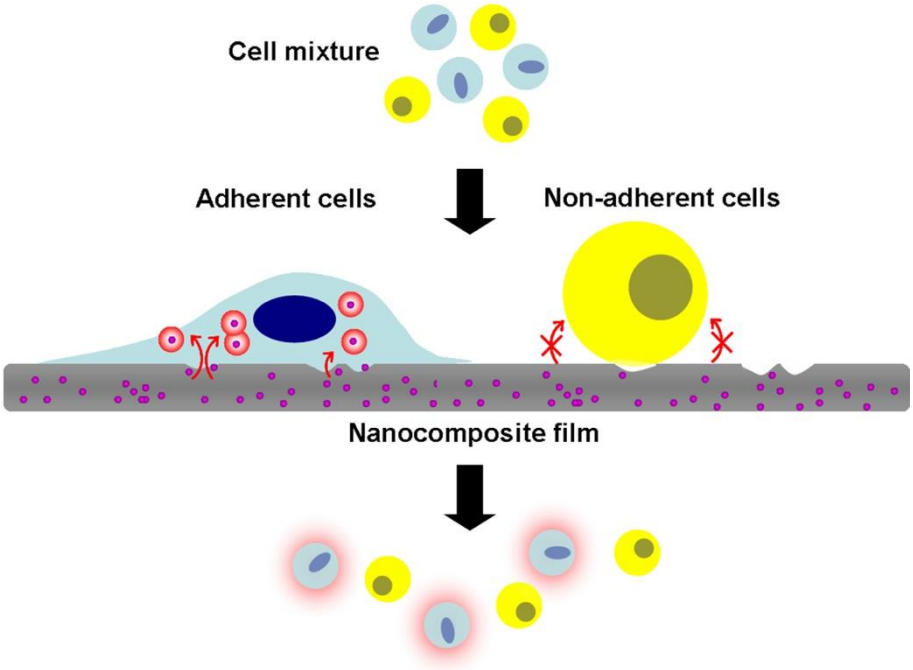
Cell mixture
Adherent cells
Non-adherent cells
Nanocomposite film